VOC Detections with Optical Spectroscopy

Yuxin Xing[1, 2], Gaoxuan Wang[1, 3, *], Tie Zhang[1], Fengjiao Shen[4],
Lingshuo Meng[5], Lihui Wang[1], Fangmei Li[1], Yuqi Zhu[3], Yuhao Zheng[3],
Nan He[1], and Sailing He[1, 2, *]

Abstract—Volatile organic compounds (VOCs or VOC) have received increasing attention recently. They are important Parameter index for air quality monitoring, and biomarkers for diseases diagnosis. For the gas sensor community, various detection technologies were explored not only to detect total VOCs, but also aim for sensor selectivity. Commercially available VOC sensors, such as metal oxide based or photoionization detectors, are suitable for total VOCs but lack of selectivity. With the advancement of optical spectroscopy, it provides a good solution for specific VOC detections. In this review, various spectroscopy techniques are summarised focusing on increasing sensor selectivity and sensitivity. The techniques considered in the paper are, non-dispersive infrared, multi-pass cell spectroscopy, cavity enhanced absorption spectroscopy, photoacoustic spectroscopy and Fourier transform infrared spectroscopy. Each technique has its advantages and disadvantages, which are also discussed.

1. INTRODUCTION

Volatile organic compounds are organic compounds with low boiling points and exist as a gas at room temperature. They can be produced by industrial, pharmaceutical and agricultural processes, emitted by plants and animals, and are responsible for water and indoor air pollutions. They also play a major role in the production of tropospheric ozone and organic aerosols through complex chemical reactions with nitrogen oxides. The detection of VOCs is vital for various purposes. For instance, VOCs produced by fungi and bacteria can be used to monitor food freshness and spoilage [1, 2]; VOCs were studied for plant evolution [3] and construction site safety [4]. Exposure to VOCs can lead to serious human health concerns, such as respiratory diseases, allergies, and immune-related effects [5]. In addition, VOCs are also important biomarkers for diseases diagnosis, such as lung cancer [6], diabetes [7], and microbial infections [8].

VOCs can be categorized based on compound volatility (very volatile, volatile and semi-volatile), and some typical examples include propane, butane, formaldehyde, ethanol, etc. Commonly, they can be monitored by devices such as metal oxide sensors, electrochemical sensors, photoionization detectors (PID) and flame ionization detectors (FID). These devices are commercially available to purchase, and even tuned to detect a specific category. Optical spectroscopy provides an alternative solution for VOC detection that is high in accuracy and resolution, with the possibility to detect multiple species at the same time. The basic principle of the optical detection system is based on the unique absorption
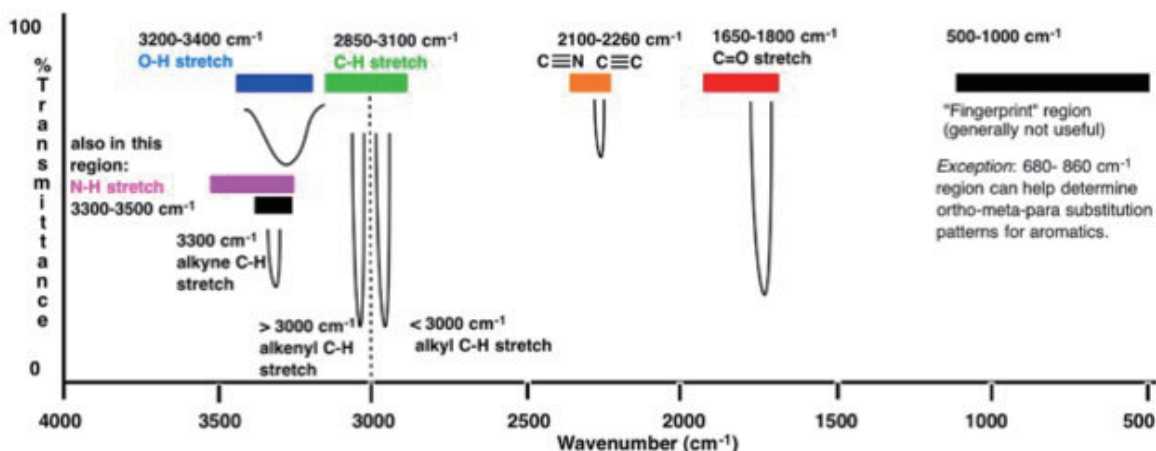
Figure 1. Typical infrared absorption windows for compounds with different molecular structures [9].

wavelengths (i.e., fingerprints) of the VOC gas molecules on the infrared spectrum, as seen in Fig. 1. It is also based on the Beer-Lambert Law, which corresponds to the relations among the transmitted light, incident light and gas cell length. In this paper, various optical spectroscopy methods are reviewed and discussed, including non-dispersive infrared, multi-pass cell spectroscopy, cavity enhanced absorption spectroscopy, photoacoustic spectroscopy, and Fourier transform infrared spectroscopy. One of the key advantages of the optical spectroscopy methods is the high selectivity (i.e., one specific gas will be target, instead of detecting similar compounds). This will also be the focus of this review.

2. SPECTROSCOPY METHODS

2.1. Non-Dispersive Infrared (NDIR)

Among all the infrared spectroscopies, non-dispersive infrared (NDIR) gas measurement is one of the simplest techniques which has been widely used for carbon dioxide detections. It is easy to implement, has lower power consumption compared to other techniques, and suitable for commercialization [10]. NDIR, as the name suggests, does not require a dispersive element or a monochromatic for gas sensing. It is commonly comprised of an infrared light source (i.e., diodes, laser, thermal emitter, etc.) and a detector (i.e., thermopile, photodiode, etc.) housed in a gas sampling chamber. Fig. 2 below shown a typical NDIR structure with the source and detector in a face-to-face arrangement.
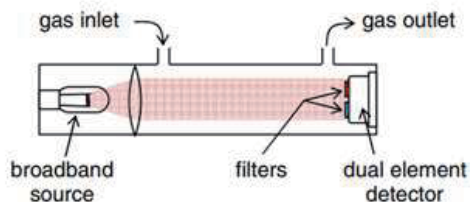
Figure 2. A typical NDIR sensing system with face-to-face emitter and detector arrangement [10].

Infrared light bulbs, with active region made of InAs [11], InAsSb [12], InAlSb [13], etc, are small and cheap. They have a broadband emission spectrum (even some with visible range) which leads to lower efficiency. Another option is a laser based setup, which provides a higher power that can be used in a bigger scale (in the unit of metres), and tunable capabilities for multiple VOC detections, examples such as [14] and [15]. More on lasers will be presented in the later sections.

Due to the applications of the NDIR system in gas sensors, low power and low cost properties are preferred. Therefore, various methods were proposed and trialled in literature on MEMS based devices to enhance radiation and absorption within a specific range. Instead of using a narrow band optical filter that overlaps with the absorption spectrum of the target gas, the source can be carefully designed to have a narrowband and highly-directional emission.

According to Kirchhoff's law, the absorptivity of an object is equal to the emissivity at thermal equilibrium. Thus, the far field thermal radiation can be controlled by tuning the absorption properties of the emitter, using resonant micro or nano structures. Generally, wave modes such as surface plasmonic polaritons (SPP) [16], gap surface plasmon (GSP) [17], or Tamm plasmon polaritons [18] are introduced to narrow the absorption bandwidth. Various subwavelength structure manipulations, such as nanoantenna [19], gratings [20], crosses [21], etc. (shown in Fig. 3) have been successfully implemented in a variety of VOC gases like acetone [22], methane [23], and ethanol [24]. Xing et al. [22] utilised cylindrical dots structure (see Fig. 4) with a narrow emission peak specifically for acetone with lower emission on the rest of the spectrum. Such designs are tunable that can also be adjusted for other gases. The design is CMOS compatible, hence low cost, and the sensor is integrated in a compact size.
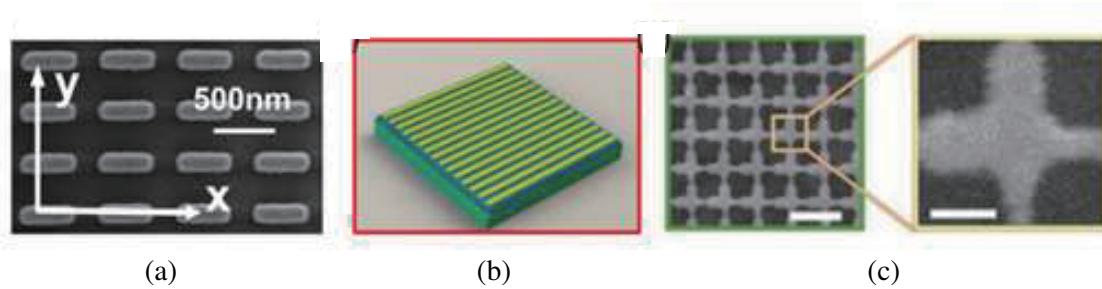

(a) (b) (c)

Figure 3. Example patterns: (a) nano antenna [19], (b) gratings [20] and (c) cross shape [21].
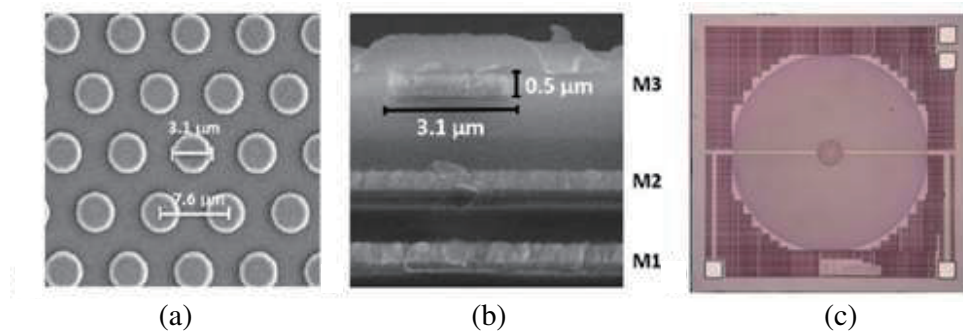

(a) (b) (c)

Figure 4. Images of the cylindrical structure: (a) magnified SEM image, (b) cross section of the device, and (c) an emitter chip [22].

Since the wavelength of the absorption will change as the angle varies (angular emission), more advanced structures, such as bull's eye structure, have been proposed and shown great selectivity and highly directional to detect C-H stretch compounds [25]. Fig. 5 shows a bull's eye structure we designed for directional thermal emission and the corresponding directional emission spectrum we simulated as the emission angle and structural period vary.

To restrict the wave to the surface of the structure, the phase matching condition should be satisfied:

$$k_g = k_{SPP} \pm k_0 \sin\theta \tag{1}$$

where k_0 is the wavevector of the emission wave in the free space; θ is the direction of the out-coupling wave; k_g is the Bragg vector; and k_{ssp} denotes the wavevector of the surface plasma polariton:

$$k_{SPP} = k_0 \sqrt{\frac{\varepsilon_m \varepsilon_d}{\varepsilon_m + \varepsilon_d}} \tag{2}$$
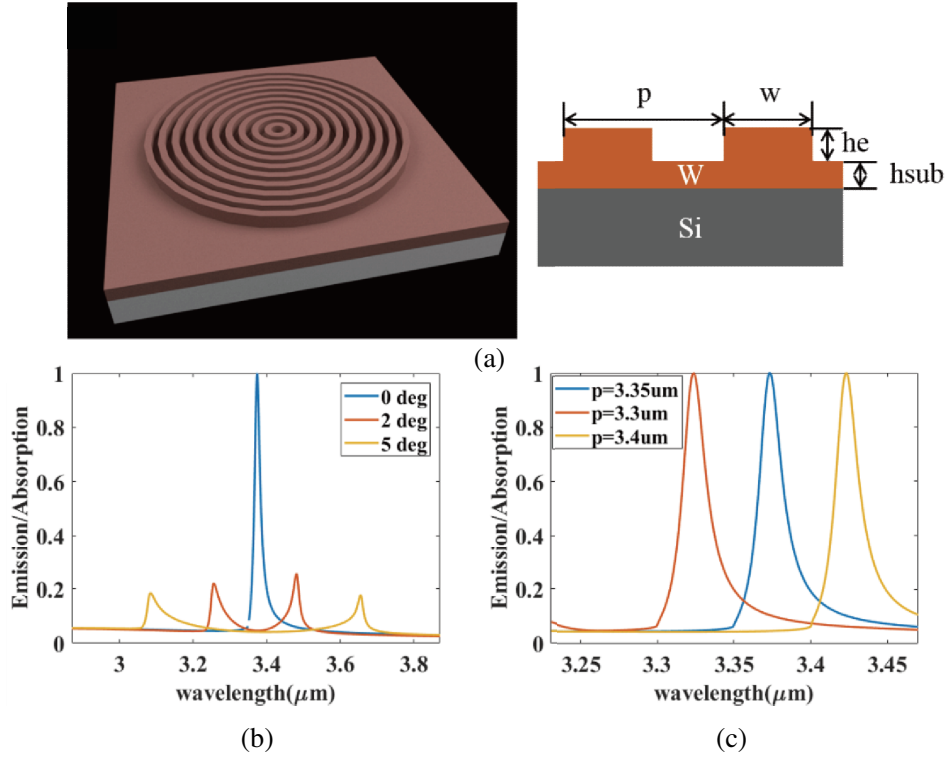
Figure 5. Narrowband high directional thermal emission by Bull's eye structure. (a) Schematic of the Bull's eye structure. The inset is the front view. (b) The emission spectrum of the structure toward different angles. (c) The emission spectrum as the period varies.

where ε_m and ε_d are the permittivities of the metal and dielectric, respectively. The circular symmetry of the Bull' eye structure ensures that the absorption, narrowed by the SPP coupling, in the normal direction is strongly enhanced, and consequently, narrowband and high directional emission is achieved.

2.2. Tunable Diode Laser Absorption Spectroscopy

2.2.1. Tunable Diode Laser Absorption Spectroscopy Based on a Multi-Pass Cell

Tunable diode laser absorption spectroscopy (TDLAS) based on the Beer-Lambert Law highly depends on the light absorption path. A multi-pass cell composed of several mirrors can effectively improve the light absorption length. A Herriott-type cell, composed of two similar spherical mirrors as a classical muti-pass cell, was widely used with the advantages of good robustness and strong practicability benefitting from its simple structure [26]. An astigmatic mirror multi-pass cell [27] is based on an astigmatic variant of the off-axis resonator (Herriott) configuration, which further improves the light absorption length. In 2017, Ozharar et al. [28] presented a novel multi-pass cavity design with the use of a rotationally symmetric end mirror as shown in Fig. 6(a). This structure can effectively increase the total number of reflections. Ta-nan et al. [29] designed a ring multi-pass optical cell consisting of three spherical mirrors to form a ring cell shown in Fig. 6(b). They designed the structure to achieve a long path length in compact volumes.

2.2.2. VOC Detection Based on Multi-Pass Cell

Amulti-pass cell can be exploited in different wavelengths from near-infrared to mid-infrared for VOCs detection. Table 1 summarized two typical VOCs (acetone and acetylene) using the TDLAS method in the wavelengths of near-infrared and mid-infrared based on different compact multi-pass cells. Acetylene is a dangerous flammable and explosive substance, and its monitoring can prevent potential
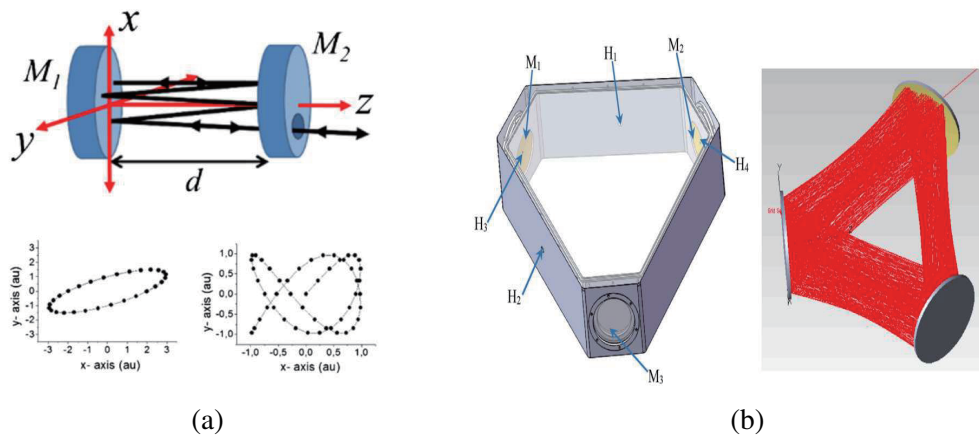
(a)   (b)

Figure 6. (a) Schematic diagram of multi-pass cell based on the use of a rotationally symmetric end mirror [28]; (b) Schematic diagram of ring multi-pass cell [29].

Table 1. Two typical VOCs (acetone and acetylene) using the TDLAS method.

VOC species	Team	Light source	Light path of MPC	Detection limit	Refs
Acetone	Nadeem	QCL (8 μm)	76 m	15 ppb	[30]
	Xia	ICL (2.97 μm)	15.8 m	120 ppb	[31]
	Schwarm	QCL (8.2 μm)	76 m	110 ppb	[32]
acetylene	Lindley	DFB (1.535 μm, 1.52 μm)	56 m	59 ppb	[33]
	Zou	DFB (1.53 μm)	21.9 m	76.75 ppb	[34]

explosion accidents. Acetone is the breath marker of diabetes and heart failure.Compact TDLAS sensors effectively complement high sensitivity measurement of VOCs in the human breath analysis.

As a typical example of VOCs detection, Zou et al. [34] demonstrated a sensitive acetylene sensing system based on a novel triple-row circular multi-pas cell as shown in Fig. 7. An Allan deviation analysis yielded a detection sensitivity of 76.75 ppb during an average time of 340 s.
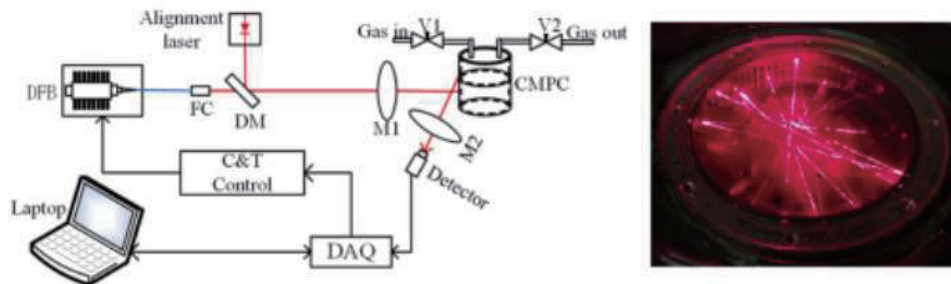
Figure 7. Schematic of the C2H2 sensor system and photograph of the triple-row CMPC [34].

As an application of the TDLAS method in the range of mid-infrared, co-author Shen et al. [35] developed a TDLAS sensor based on a continuous-wave external-cavity quantum cascade laser (EC-QCL) operating in 8 μm for real-time on-line monitoring of N2O.The TDLAS method can remotely monitor the trace gas concentration as reported by He et al. [36]. A compact remote sensor for measuring the methane concentration was developed based on the tunable diode laser absorption spectroscopy as shown in Fig. 8 and validated by field monitoring of methane emissions at a large-scale landfill in China.

Figure 8. The framework of the gas concentration testing system [34].

2.3. Cavity Enhanced Spectroscopy
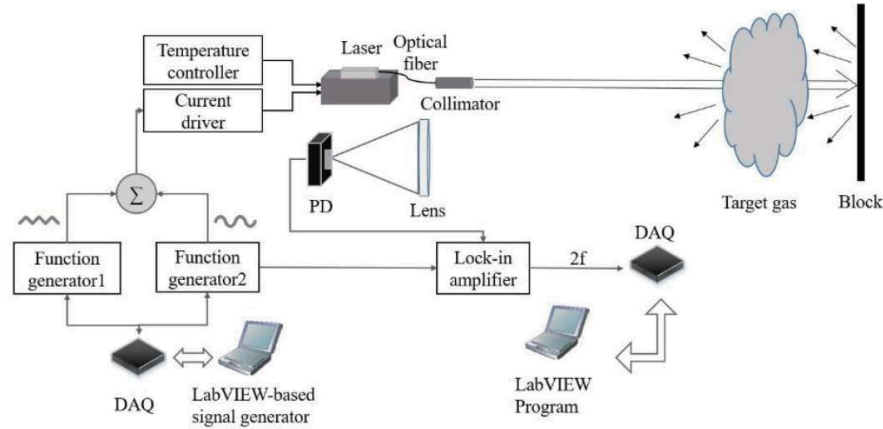
To increase the light absorption path length, cavity enhanced techniques based on high finesse optical cavities were proposed for VOCs detection, such as cavity ring-down spectroscopy (CRDS) and Incoherent Broadband Cavity-Enhanced Absorption spectroscopy (IBBCEAS). The effective absorption optical path length is improved by multiple reflections of light in a finite-length resonant cavity, thereby greatly improving the detection sensitivity [37–39].

2.3.1. Cavity Ring-Down Spectroscopy(CRDS)

In **CRDS**, light intensity leaking out from the cavity decreases exponentially. The measurements of the ring-down times with and without the VOCs sample (denoted by τ and τ_0, respectively) inside the cavity allow one to deduce the absorption coefficient $\alpha_{\text{ext}}(\lambda)$ of VOCs sample as shown in Fig. 9 [40]:

$$\alpha_{\text{ext}}(\lambda) = \frac{1}{c}\left(\frac{1}{\tau} - \frac{1}{\tau_0}\right) \tag{3}$$

where c is the speed of light in vacuum. When the light intensity reaches a set threshold, the light source is quickly cut off. The laser light remaining in the cavity is continuously reflected in the high finesse cavity, and the intensity of the transmitted light in the cavity decays exponentially. As shown in Fig. 9(b), a background or reference measurement of the decay time (τ) is required. For ring-down cavities containing the sample, the light intensity decay is accelerated due to the absorption by the sample as well as the additional losses (absorption and scattering by impurity gases). The concentration of the substance to be tested can be determined by measuring and calculating the ring-down time τ in the cavity and the ring-down time τ when the cavity contains the sample.

Since its first demonstration by O'Keefe and Deacon in 1988 [39] the CRDS technique has been widely used for sensitive measurement of trace gases including VOCs species such as acetylene, ethylene, methyl-iodide, dimethyl and disulfide, etc. Table 2 summarizes some CRDS instruments developed for VOCs species measurements in a wavelength range from 266 to 3235 nm. Diode lasers and Nd: YAG laser are widely used withan FWHM (full width at half maximum) less than 1 nm to avoid as much as possible the interference from other gases.

For improving the sensitivity of the device, Parkes' group and Pradhan's group adopted some methods to pre-concentrate the samples, and improved the detection limits of ethylene and acetylene to 200 ppt [41] and 35 ppt [42], respectively; Wang's team developed the first CRDS-based acetone breath analyzer with a detection limit of 0.13 ppm [43]; Bicer's team used a DFB laser to achieve multi-component gas detection with detection limits of 8 ppb and 2.1 ppb for methane and acetone, respectively [44]; The team of I. Sadiek achieved the measurement of methyl iodide in the mid-infrared band with a detection limit of 15 ppb, and there is still room for improvement [45]. The Wang's
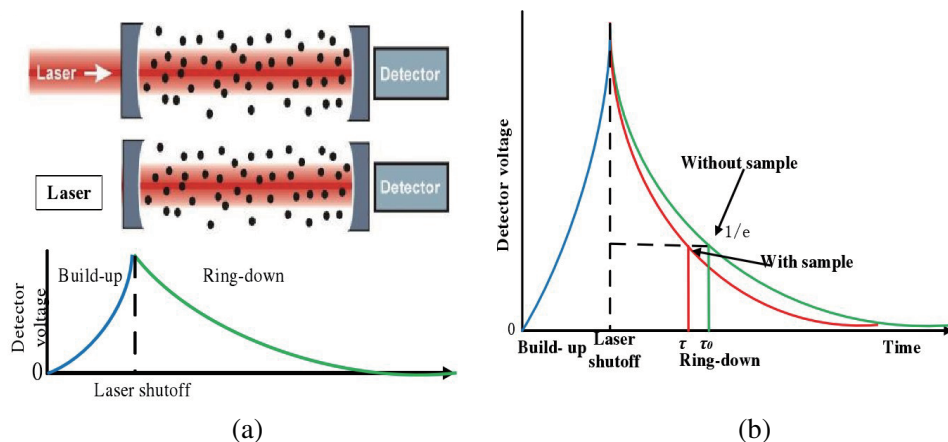
Figure 9. (a) Schematic diagram of the cavity ring-down spectroscopy; (b) Schematic diagram of the light intensity attenuation in the cavity [40].

Table 2. Some CRDS instruments developed for VOCs species measurements in a wavelength range from 266 to 3235 nm.

Team	Light source	VOC species	Wavelength (nm)	Detection limit	Refs
A.M.Parkes	Diode laser	acetylene,ethylene	1519.67, 1625.94	6 ppb,200ppt	[41, 47]
M. Pradhan	Diode laser	acetylene	1535.393	35 ppt	[42]
F. M. Schmidt	Diode laser	acetylene	1523	340 ppt	[48, 49]
C. Wang	pulsed laser	acetone	266	0.13 ppm	[43]
A. Bicer	Diode laser	methane, acetone	1671	8 ppb, 2.1 ppb	[44]
I. Sadiek	DFB laser	methyl iodide	3235.79	15 ppb	[45]
Z. Wang	Nd: YAG laser	Dimethyl Disulfide	266	ppm-ppt	[46]

team reported the first measurement of CRDS-based dimethyl disulfide, demonstrating the feasibility of developing a portable melanoma screening sensor using the CRDS technology [46].

Figure 10 shows the CW-CRDS device built by Pradhan's team. They further improved the detection limit of acetylene to 35 ppt [42] by combining continuous wave cavity ring-down spectroscopy with sample pre-concentration, which is sufficient for direct atmospheric detection of C_2H_2 at typical concentrations of both urban and rural environments.
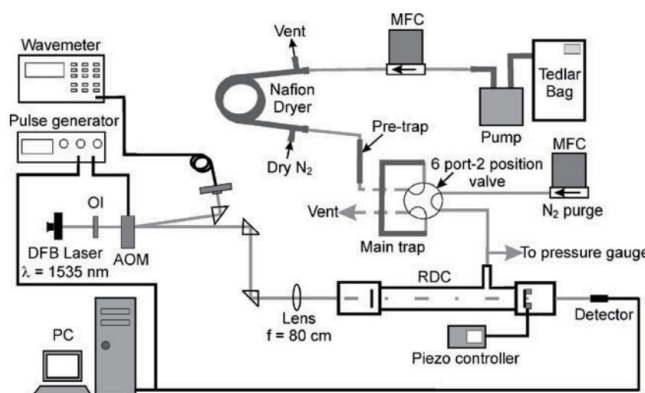

Figure 10. Schematic diagram of the experimental setup [42].

2.3.2. Incoherent Broadband Cavity-Enhanced Absorption Spectroscopy (IBBCEAS)

Narrow-band CRDS measurements could not provide accurate VOCs detection in broad band wavelength range. IBBCEAS instrument using a broad-band light emitting diode (LED) or Xe lamp as a light source offers a capability of broadband detection. At the same time, the use of an incoherent broadband light source eliminates the issue of the mode matching between the optical cavity and the light source. The optical absorption coefficient $\alpha(\lambda)$ of the particulate sample measured by IBBCEAS can be expressed as [50, 51]:

$$\alpha(\lambda) = \left(\frac{1 - R(\lambda)}{L} + \alpha_{Ray}(\lambda) \right) \times \left(\frac{I_0(\lambda) - I(\lambda)}{I(\lambda)} \right) \tag{4}$$

where $R(\lambda)$ is the mirror effective reflectivity; L is the cavity length; $I(\lambda)$ and $I(\lambda)$ are the light intensities transmitted through the cavity without and with the sample, respectively. $\alpha_{\mathrm{Ray}}(\lambda)$ is the Rayleigh scattering coefficient of gases. The IBBCEAS technique was first proposed by Fiedler et al. in 2003 to measure the absorption spectra of oxygen (O2) and gaseous chamomile cyclic hydrocarbons (C10H8) around the wavelength of 630 nm using an incoherent broadband light source short-arc xenon lamp and a CCD spectrometer [52, 53].

An incoherent broadband light source, as a key element in an IBBCEAS system, could be a xenon lamp, a laser-driven plasma light source (LDLS) or an LED. The broadband wavelength range emitted by a xenon lamp is mainly concentrated in 200 nm to 800 nm, but with disadvantages of large volume, low optical coupling efficiency, high price and high-power consumption. A laser-driven plasma light source is a new type of broadband light source. It uses a continuous-wave laser to directly heat a neon gas plasma to a temperature of 20000 K, thereby emitting broadband radiation [54]. An LDLS is a smaller, more stable and high-brightness plasma-emitting point source that can be efficiently coupled into an optical system, with a spectral range from 170 nm–2100 nm, especially in the ultraviolet and deep ultraviolet spectral range [54]. The spectral shape of the LED is generally similar to the Gaussian type, the full width at half maximum is about ten or tens of nanometers, and the power consumption is low. It is also often used in an IBBCEAS system [51, 55, 56].

Table 3 summarizes some IBBCEAS instruments developed for VOCs measurements inultraviolet-visible-infrared spectrum using some supercontinuum source, xenon lamps, laser-driven plasma light sources (LDLS) and LEDs for detection of $C_{10}H_8$, C_4H_6, $C_4H_8O_2$, VOCs from photolysis of 2-introphenol, CH_2O and $C_2H_2O_2$.

Table 3. Some IBBCEAS instruments developed for VOCs measurements.

Team	Light source	VOCs species	Wavelength	LoD (Mm^{-1})	Refs
Fiedler	Xe lamp	$C_{10}H_8$	630 nm		[52]
Denzer	SLED	1,3-Butadiene (C_4H_6)	1600–1700 nm	1.5 Mm^{-1}	[57]
Chandran	Xe lamp	1,4-Dioxane ($C_4H_8O_2$)	1215–1695 nm	8 Mm^{-1}	[58]
Denzer	Supercontinuum source, SLED, Xe lamp	C_2H_2	1500–1700 nm	0.4 Mm^{-1}	[59]
Amiot	Supercontinuum source	CH_4, C_2H_2	3000–3450 nm	2 ppm (C_2H_2)	[60]
Fang	blue LED	Glyoxal (CHOCHO)	440–480	0.59 Mm^{-1}	[61]
Venables	LED	VOCs from photolysis of 2-introphenol	300–400 nm	2 Mm^{-1}	[62]
Chen	LED	CH_2O HONO	350–380	41 ppbv for CH_2O	[63]

Glyoxal (CHOCHO), the simplest α-dicarbonyl group, exists in the atmosphere as a primary derivative of VOCs and leads to the formation of secondary organic aerosols (SOA) and ozone (O3). Although CHOCHO plays an important role in SOA formation and photochemistry, techniques for rapid and in situ measurement of atmospheric CHOCHO remain scarce so far. Fang et al. developed a highly sensitive IBBCEAS system (Fig. 11(a)) using a customized cage structure and a 42 cm-long cavity to achieve sensitive, real-time, in-situ measurements of CHOCHO and NO2 in the spectral range of 440–480 nm as shown in Fig. 11(b) [61].

VOCs species have abundant unique absorption information in the UV band. The group of Venables detect VOCs from the photolysis of 2-nitophonel and monitored the absorption cross section of 2-nitrophenol in the wavelength range of 300450 nm Simulation chamber is a powerful tool to study the chemical reaction of VOCs. The group of Chen installed an IBBCEAS sensor with the range of 350 nm
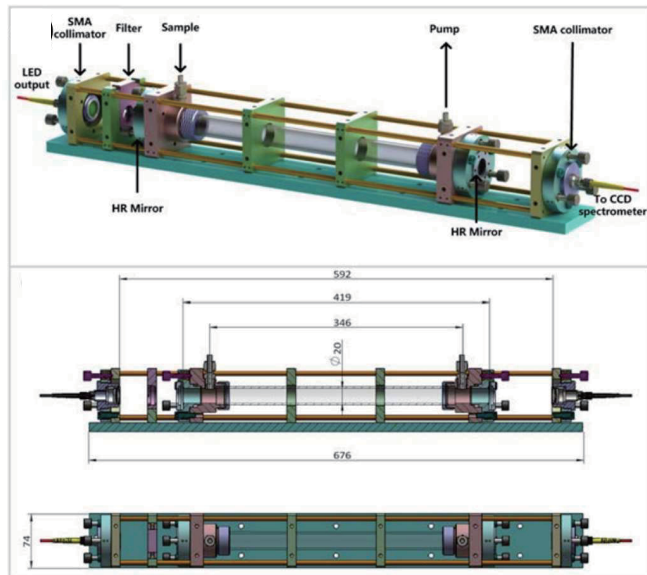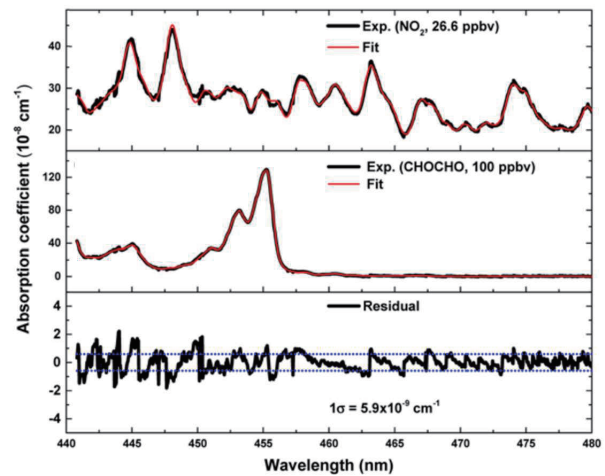
(a)   (b)

Figure 11. (a) Schematic diagram of the cage cavity-based IBBCEAS device, enabling a compact and easy-to-align optical system; (b) the measured NO2 and CHOCHO absorption spectra and their fitting results [61].
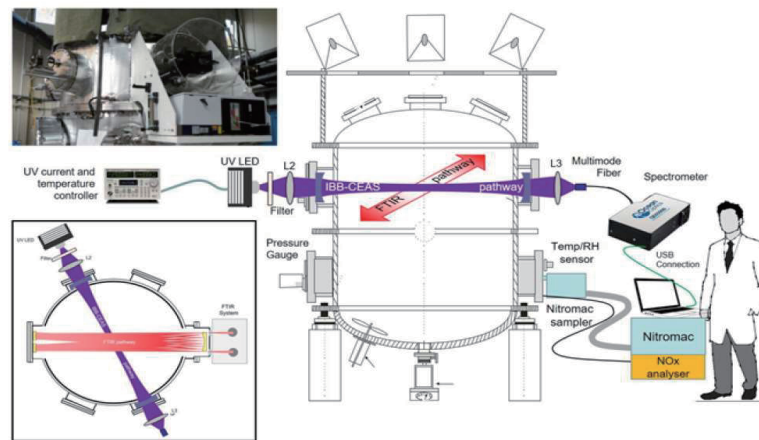

Figure 12. Schematics BBCEAS sensor installed in a simulation chamber [63].

to 380 nm in a simulation chamber for detection of CH2O, HONO, and NO2 compared with a Fourier transform infrared (FTIR) spectrometer as shown in Fig. 12 [63]. Co-author Meng from the group of Chen also demonstrated the feasibility of IBBCEAS sensor shown in Fig. 13 in measurement of aerosol (containing VOCs) in the ranging (lidar) blind zone (i.e., the firsthundreds of meters of the observation range) [64].
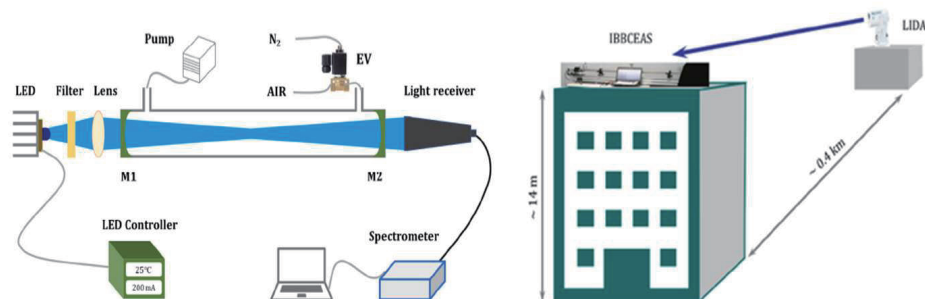

Figure 13. Schematic of combined BBCEAS sensor near the ground surface in the ranging (lidar) blind zone [52].

2.4. Photoacoustic Spectroscopy

2.4.1. Principle of Photoacoustic Spectroscopy

Photoacoustic spectroscopy is based on the detection of acoustic signals resulting from the light absorption of a modulated laser radiation by the target species. The photo-acoustic (PA) effect converts the absorbed photon energy into acoustic sound, that was discovered by Alexander Graham Bell in 1880 [65]. The PA effect in gases can be divided into three main steps as shown in Fig. 14 [66]:

(1) Localized heat release in the sample gas by absorption of the incident laser radiation at a wavelength that overlaps with a spectral feature of the target species.
(2) Energy expansion and contraction processes: acoustic and thermal wave generation due to the localized transient heating and expansion;
(3) Detection of the acoustic signal in the PA cell with a microphone.
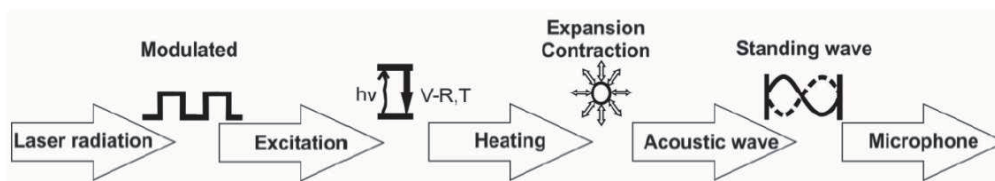
Figure 14. Schematic of photoacoustic effect process [66].

2.4.2. Different Structure of PA Spectrometer for Detection of VOCs

Different acoustic transducers can be used for detection of acoustic signals, including condenser and electret microphones, quartz tuning forks (QTF), micromachined cantilevers and other microelectromechanical system (MEMS) devices [67, 68].

The light absorption of VOCs is not a Lorentzian profile, which is the most suitable condition for optical gas spectroscopy. For complex molecules, the light absorption is companied by the broadening of absorption lines, resulting from the structured absorption features over a wide spectral range, thus increases the difficulty in the detection of VOCs [69]. A wide-tunability is required to detect VOCs in

complex gas mixtures. Such widely tunable high-power lasers that are currently available, includes CO and CO2 lasers, optical parametric oscillators (OPOs), and external cavity quantum cascade lasers (EC-QCLs) [66]. Different combination schemes of acoustic transducers with widely tunable light sources for the detection of VOCs have also been reported.

The most widely used transducer in PA spectroscopy is condenser and electret microphones with advantages of low power consumption, high sensitivity and low noise level. CO2 laser has the advantages of high power and having multiple laser lines in the 9–11 μm infrared region. Thus, a CO2 laser photoacoustic spectrometer (PAS) companied with condenser and electret microphones can have a multi-component measurement capability for measuring several VOCs in the human breath [66]. Popa et al. have achieved five components measurement using a CO2 laser PAS system coupled with electret microphones for detecting carbon dioxide, ammonia, ethanol, methanol, and ethylene, in a mouth breathing versus nasal breathing study [70]. Mitrayana et al. built a CO2 laser photoacoustic spectrometer as shown in Fig. 15 for measuring ammonia, acetone, and ethylene trace gases in breath samples from 10 renal disease patients [71].
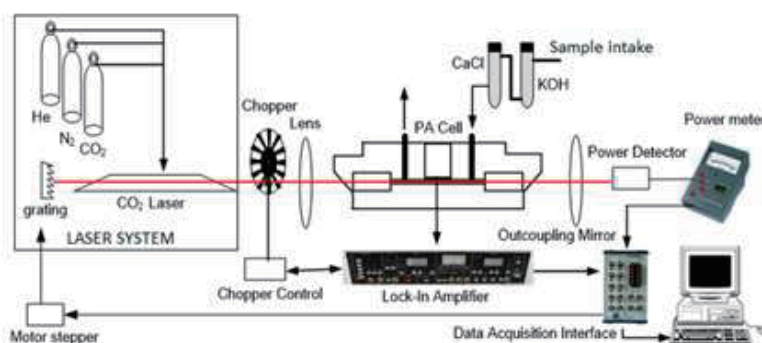

Figure 15. Schematic of the CO2 laser photoacoustic spectrometer [71].

Chlorinated hydrocarbons, as important VOCs in the industrial activities from foam plastic products and pharmaceuticals production, are of concern as toxic air pollutants and carcinogen species. Mohebbifar used a CO2 laser in a wavelength range of 877 to 1086 cm^{-1} to realize a single species of $CHCl_3$ measurement with a sensitivity of 488 ppbv [72]. Our group have developed a compact photoacoustic (PA) spectrophone (Fig. 16) based on electret microphones for simultaneous detection of trichloromethane ($CHCl_3$) and dichloromethane (CH_2Cl_2) by employing a low-cost distributed feedback (DFB) laser emitting at 1684 nm. Continuous monitoring of Chloroform Gas with a high detection sensitivity of 280 ppbv was achieved [73, 74].

Quartz tuning fork (QTF) with a very high Q factor ($\sim$ 10000 at atmospheric pressure) is an alternative transducer for acoustic signal measurements. It converts mechanical displacement (caused by acoustic signal) into a readable electrical signal, commonly referred to as quartz-enhanced photoacoustic spectroscopy (QEPAS) [75]. Recently, Ayache et al. presented a QEAPS sensor dedicated to benzene detection by exploiting a 14.85 μm quantum cascade laser. This benzene sensor has a good selectivity and a limit of detection of 30 ppbv in 1 s [76].

Unlike the traditional QEPAS method based on the photoelectric effect, quartz-tuning-fork enhanced photothermal spectroscopy (QEPTS) utilizes the piezoelectric effect and resonance effect of the QFT to gauge the light intensity [14, 77–79]. The transmitted laser light was vertically focused onto the surface of the QCTF prongs. QEPTS is a non-contact measurement technique and can be used for remote trace gas detections. Ma et al. developed a QEPTS sensor for acetylene (C_2H_2) detection using a 1.53 μm continuous wave distributed feedback (CW-DFB) diode laser, which achieved a minimum detection limit (MDL) of 718 ppbv [77]. Liu et al. reported a remote sensor based on QCTF coupling to a broadband tunable external cavity quantum cascade lasers (ECQCLs) for detection of three VOCs mixing plume (i.e., ethanol, acetone and diethyl ether) at a distance of 40 m in Fig. 17, proving its applicability for leak plumes in security fields [14].

Micromachined cantilever method can be used in PA spectrophone as PA signal transducer, also
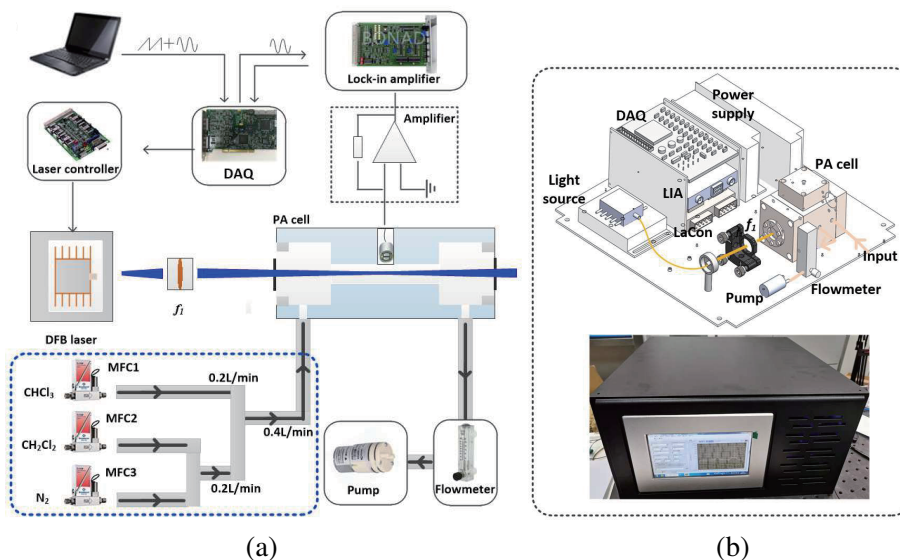
(a)   (b)

Figure 16. (a) Schematic view of the compact PA spectrophone [73]. (b) The developed compact photoacoustic sensing system and its internal construction. DAQ: data acquisition card, MFC: mass flow controller, LIA: lock-in amplifier, LaCon: laser controller, f1: focus lens.
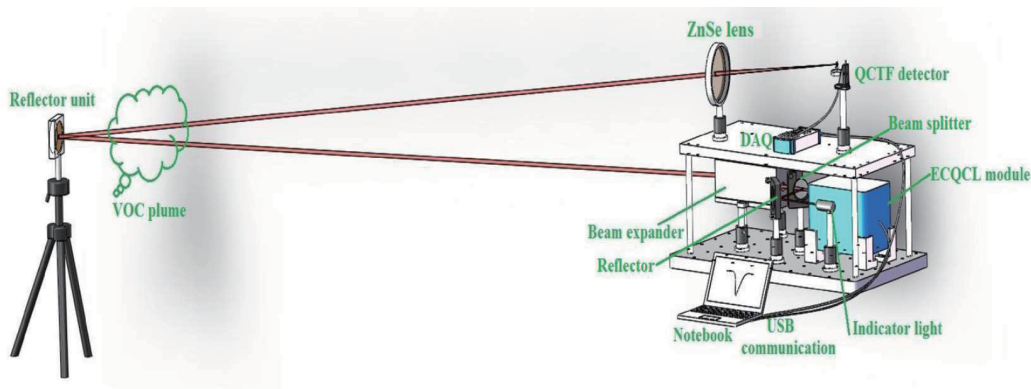

Figure 17. Schematic of a remote sensor based on QCTF and ECQCL [14].

known as cantilever enhanced photo-acoustic spectroscopy (CEPAS). CEPAS can detect very low gas concentrations with detection limits demonstrated at parts-per-trillion (ppt) level or lower [80]. CEPAS has been applied to measure various volatile organic compounds. Karhu et al. reported a novel CEPAS sensor for trace gas sensing of benzene using a quantum cascade laser emitting at the wavelength 14.8 mm, and a benzene detection limit below 1 ppb was achieved [81]. Hirschmann et al. validated a new photoacoustic FTIR system installed with a cantilever microphone and realized a detection of five VOCs including acetone, methanol, perchloroethylene, methyl isobutyl ketone and dimethylformamide [82].

A growing interest in PAS for the 2.5–5 μm region is represented by optical parametric oscillators (OPO) with advantages of high power (several watts) level, narrow linewidth and wide-range wavelength tunability [66]. Saalberg et al. developed a sensor based on PAS for six VOCs (2-butanone, 1-propanol, isoprene, ethylbenzene, styrene, and hexanal) that are linked to lung cancer, by exploiting an OPO radiation source in a wavelength region from 3.2 μm to 3.5 μm shown in Fig. 18. The detection limit for a single substance of the PA sensor was between 5 ppb and 142 ppbv [83].
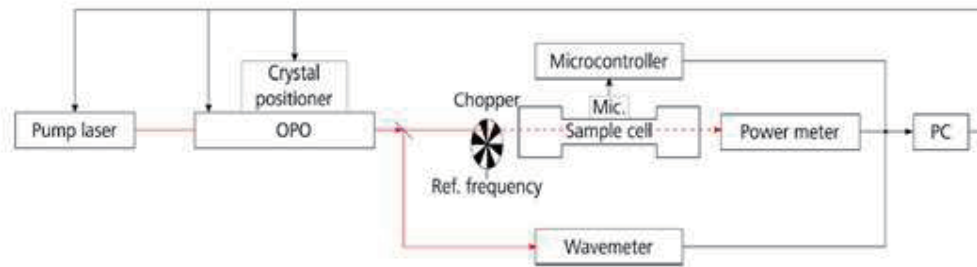
Figure 18. Experimental setup of PA sensor coupled to OPO radiation source [83].

2.5. Fourier Transform Infrared (FTIR) Spectroscopy

Fourier transform infrared (FTIR) spectroscopy is a method to acquire the infrared spectrum by Fourier transforming the interferogram, and there is a functional relationship between the intensity of the infrared (IR) spectrum and the optical path difference of the two coherent beams. Owing to its significant advantages in signal-to-noise ratio (SNR) and resolution, FTIR has been the dominant technique used for measuring the IR absorption and emission spectra in recent decades. Most of the gases show characteristic absorption in the IR region so that they can be quantitatively and qualitatively analyzed by taking the advantage of the FTIR technique.Compared with other optical sensing technologies, the wide spectral coverage of FTIR meets the needs of simultaneous measurement of dozens of gases, and the deterioration of the environmental has promoted the progress of FTIR technology in the field of atmospheric trace gas monitoring since the 1970s, and much progress in VOCs detection based on FTIR technique have been achieved nowadays.

The FTIR measurement methods can be divided into extractive and open path measurements [84]. The extractive measurements of FTIR spectroscopy include extracting a sample stream of gases from a certain location, transporting it to an IR absorption cell and isolating it for analysis [85]. In order to detect trace VOCs, improvements for the gas cell have been made to increase the effective length of the optical path, so as to achieve the detection range of sub parts per million [86], and therefore, small multi-pass cells are popular in the extractive measurements [87]. By combining the extractive measurement FTIR technology with traditional Gas Chromatography/Mass Spectrometry (GC/MS) technology, hundreds of VOCs can be accurately measured at the same time [88].

Open-path FTIR (OP-FTIR) has been developed rapidly in recent years due to its suitability for analytical tasks that cannot be performed adequately by using analytical methods based on point sampling. The OP-FTIR spectroscopy relies on the external IR source, such as the sun or natural hot objects as IR sources for radiation, and calculates the integrated concentration of gases over a long path in the field. The OP-FTIR is commonly used in monitoring production and domestic emissions [89–91]. There are two ways to perform open-path measurements, namely, active and passive measurement techniques according to the difference of the IR sources. The active measurement method is rarely affected by the changes of the external environment, and can ensure all-weather measurement. A typical system structure of active measurement diagram is depicted in Fig. 19 [92]. An infrared laser or a thermal radiation light source is usually used as the emission light source. The reflected light is collected by a telescope system and input into the FTIR for demodulation.MCT is usually used as the detector in the FTIR, because of its outstanding response in mid infrared band [93]. If conditions permit, the IR source and FTIR can be placed tens of meters apart to detect the gas on the path [94, 95].

Because of the limitations of man-made IR sources in power and size, people gradually turn to the sun as the light source for passive measurement. This method can directly detect the gas concentration at the vertical height, which is of great significance for monitoring the atmospheric environment. Fig. 20 shows the vertical distribution of ethylbenzene and m-xylene in Shijiazhuang, China [96].

Regardless of which FTIR measurement method is adopted, it faces various difficulties related to the collection of appropriate background reference spectra, the ways of qualitative analysis and quantitative evaluation of measured spectra, the problems of calibration, and the effects of spectral resolution on the detection sensitivity.
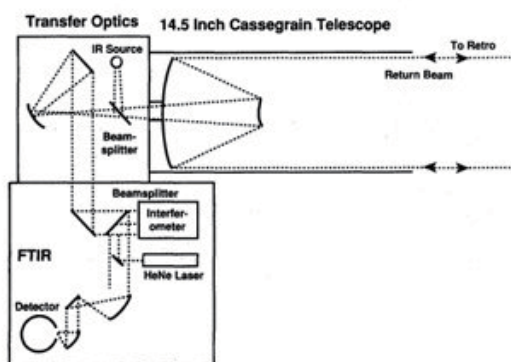
Figure 19. Schematic of active OP-FTIR system [92].
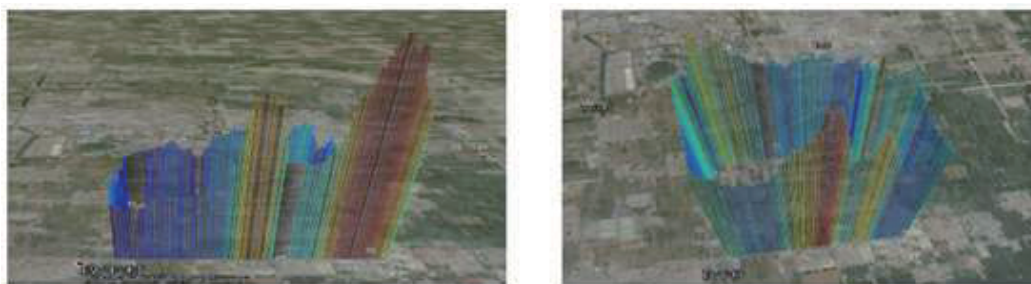
Figure 20. The distribution of ethylbenzene and m-Xylene [96].

2.6. Laser Absorption Spectroscopy Coupled to Gas Chromatography

Gas chromatography — mass spectrometry (GC-MS), as the 'gold standard technique' for trace gas analysis, has become a common method used for the study of VOCs. However, GC-MS instruments are laboratory-based and not directly suitable for mobile operations [97, 98]. Photoionization or flame ionization coupled to GC gives more compact setups but lowers the sensitivity and selectivity [98]. The application of laser absorption spectroscopy (LAS) as a GC detector could offer new possibilities to analytical chemistry.

Zare et al. coupled a standard cavity ring-down spectrometer (CRDS) to a gas chromatograph through a combustor (resulting in the analysis of 13C/12C isotope ratios of organic compounds)

Figure 21. Schematic picture of GC-PAS system [98].

and validated by the detection of 13C/12C isotope ratios of methane, ethane, and propane [99]. Recently, Tomberg et al. coupled a cantilever enhanced photo-acoustic spectrophone with a GC for compound separation and with a widely tunable external-cavi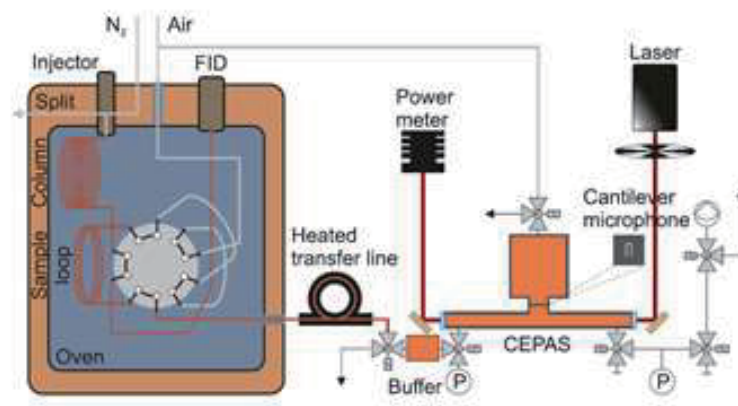ty quantum cascade laser for compound identification in the optical fingerprint region shown in Fig. 21 [98]. The GC-PAS system offers considerable advantages for analyzing complex mixtures of large molecules including cyclohexane, 1-Propanol, Isobutanol, 1-Pentanol, 1-Hexanol, Methanol, ethanol and 2-Ethyl-1-Hexanol, as shown in Fig. 22.
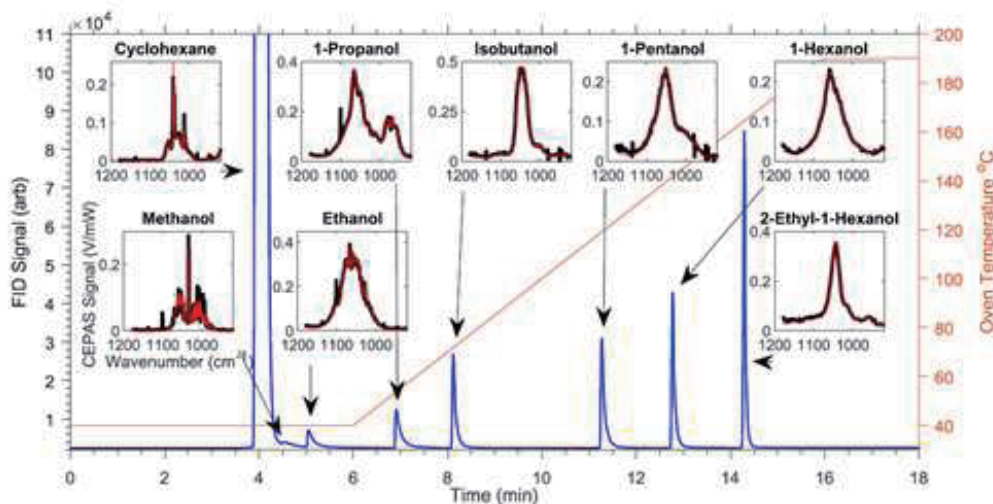

Figure 22. Sample chromatogram (left vertical axis) and the corresponding oven program (right vertical axis). The insets show the corresponding optical-power-normalized CEPAS detector signal (spectra) for each peak. The black traces are the measured data and the red traces are fits to the data from the PNNL database [99].

3. CONCLUSION

In this review paper, various absorption spectroscopy methods for VOCs detection have been summarized, including NDIR, multi-pass cell method, cavity enhanced absorption spectroscopy, photoacoustic spectroscopy, and Fourier transform infrared spectroscopy. Laser absorption spectroscopy follows an exponential law with the optical absorption length. Various methods have been implemented for improving the sensitivity and selectivity of spectroscopic measurements.

Although the short light path in NDIR leads to low sensitivity, the simple light path structure makes it suitable for commercialization with advantages of low cost and CMOS compatibility (can be integrated in a compact size). A multi-pass cell can increase the optical path through dozens or hundreds of light reflections within a limited space composed of several mirrors. High reflectivity mirrors are used in cavity enhanced techniques such as CRDS, IBBCEAS and ICOS to form an optical cavity of high finesse. The light trapped in the cavity bounces back and forth between the cavity mirrors several hundred thousand times to give an effective optical length of up to several kilometers. However, the above methods are limited by the narrow band of the photodetector. Photoacoustic spectroscopy is based on the generation of acoustic signals from the light absorption of certain targeted gas molecules with the advantages of independence of the light wavelength. FTIR spectroscopy is a method to acquire the infrared spectrum by Fourier transforming the interferogram with the advantages of wide spectral coverage.

Due to various structured light absorptions of VOCs in a broad spectrum, a wide-tunable radiation source is required to detect VOCs in complex gas mixtures, such as CO_2 lasers, optical parametric oscillators (OPOs), or external cavity quantum cascade lasers (EC-QCLs). Different combinations of laser absorption spectroscopy (LAS) with broadband light sources have been reported for detection

of VOCs in the monitoring of air quality or breath analysis. The combination of LAS with gas chromatography provides a new possibility for VOCs detection, and guarantees the identification and quantification of multi-species in the meantime. In conclusion, the LAS method can be exploited and satisfy almost all requirements in different applications with the advantages of portability, high sensitivity, and multi-species analysis.

ACKNOWLEDGMENT

REFERENCES

1. Inamdar, A. A., S. Morath, and J. W. Bennett, "Fungal volatile organic compounds: More than just a funky smell?" *Annual Review of Microbiology*, Vol. 74, No. 1, 101–116, 2020, doi: 10.1146/annurev-micro-012420-080428.

2. Sater, H. M., L. N. Bizzio, D. M. Tieman, and P. D. Muñoz, "A review of the fruit volatiles found in blueberry and other vaccinium species," *Journal of Agricultural and Food Chemistry*, Vol. 68, No. 21, 5777–5786, May 27, 2020, doi: 10.1021/acs.jafc.0c01445.

3. Picazo-Aragonés, J., A. Terrab, and F. Balao, "Plant volatile organic compounds evolution: Transcriptional regulation, epigenetics and polyploidy," *Int. J. Mol. Sci.*, Vol. 21, No. 23, November 25, 2020 (in English), doi: 10.3390/ijms21238956.

4. Wang, M., C. Wang, S. Huang, and H. Yuan, "Study on asphalt volatile organic compounds emission reduction: A state-of-the-art review," *Journal of Cleaner Production*, Vol. 318, 128596, October 10, 2021, doi: https://doi.org/10.1016/j.jclepro.2021.128596.

5. Nurmatov, U., N. Tagieva, S. Semple, G. Devereux, and A. Sheikh, "Volatile organic compounds and risk of asthma and allergy: A systematic review and meta-analysis of observational and interventional studies," *Prim. Care. Respir. J.*, Vol. 22, No. 1, 9–15, March 2013 (in English), doi: 10.4104/pcrj.2013.00010.

6. Hua, Q., Y. Zhu, and H. Liu, "Detection of volatile organic compounds in exhaled breath to screen lung cancer: A systematic review," *Future Oncol.*, Vol. 14, No. 16, 1647–1662, July, 2018 (in English), doi: 10.2217/fon-2017-0676.

7. Novak, B. J., D. R. Blake, S. Meinardi, F. S. Rowland, A. Pontello, D. M. Cooper, and P. R. Galassetti, "Exhaled methyl nitrate as a noninvasive marker of hyperglycemia in type 1 diabetes," *Proc. Natl. Acad. Sci. U S A*, Vol. 104, No. 40, 15613-8, October 2, 2007 (in English), doi: 10.1073/pnas.0706533104.

8. Ahmed, W. M., O. Lawal, T. M. Nijsen, R. Goodacre, and S. J. Fowler, "Exhaled volatile organic compounds of infection: A systematic review," *ACS Infect. Dis.*, Vol. 3, No. 10, 695-710, October 13, 2017 (in English), doi: 10.1021/acsinfecdis.7b00088.

9. Ashenhurst, J., *Infrared Spectroscopy: A Quick Primer On Interpreting Spectra*, 2016.

10. Hodgkinson, J. and R. P. Tatam, "Optical gas sensing: A review," *Measurement Science and Technology*, Vol. 24, No. 1, 012004, November 28, 2012, doi: 10.1088/0957-0233/24/1/012004.

11. Krier, A., M. Yin, V. Smirnov, P. Batty, P. J. Carrington, V. Solovev, and V. Sherstnev, "The development of room temperature LEDs and lasers for the mid-infrared spectral range," *Physica Status Solidi (A)*, Vol. 205, No. 1, 129–143, 2008, doi: https://doi.org/10.1002/pssa.200776833.

12. Alexandrov, S., G. A. Gavrilov, A. A. Kapralov, S. A. Karandashev, B. A. Matveev, G. Y. Sotnikova, and N. M. Stus, "Portable optoelectronic gas sensors operating in the mid-IR spectral range (lambda = 35 μm," *Second International Conference on Lasers for Measurement and Information Transfer. SPIE*, 2002.

13. Haigh, M. K., G. R. Nash, S. J. Smith, L. Buckle, M. T. Emeny, and T. Ashley, "Mid-infrared AlxIn1-xSb light-emitting diodes," *Applied Physics Letters*, Vol. 90, No. 23, 231116, 2007, doi: 10.1063/1.2745256.

14. Liu, N., S. Zhou, L. Zhang, B. Yu, H. Fischer, W. Ren, and J. Li, "Standoff detection of VOCs using external cavity quantum cascade laser spectroscopy," *Laser Physics Letters*, Vol. 15, No. 8, 085701, June 6, 2018, doi: 10.1088/1612-202x/aac356.

15. Ciaffoni, L., G. Hancock, J. J. Harrison, J.-P. H. van Helden, C. E. Langley, R. Peverall, G. A. D. Ritchie, and S. Wood, "Demonstration of a mid-infrared cavity enhanced absorption spectrometer for breath acetone detection," *Analytical Chemistry*, Vol. 85, No. 2, 846–850, January 15, 2013, doi: 10.1021/ac3031465.

16. Qu, Y., Q. Li, H. Gong, K. Du, S. Bai, D. Zhao, H. Ye, and M. Qiu, "Spatially and spectrally resolved narrowband optical absorber based on 2d grating nanostructures on metallic films," *Advanced Optical Materials*, Vol. 4, No. 3, 480–486, 2016, doi: https://doi.org/10.1002/adom.201500651.

17. Kang, S., Z. Qian, V. Rajaram, S. D. Calisgan, A. Alù, and M. Rinaldi, "Ultra-narrowband metamaterial absorbers for high spectral resolution infrared spectroscopy," *Advanced Optical Materials*, Vol. 7, No. 2, 1801236, 2019, doi: https://doi.org/10.1002/adom.201801236.

18. Wang, Z., J. K. Clark, Y.-L. Ho, S. Volz, H. Daiguji, and J.-J. Delaunay, "Ultranarrow and wavelength-tunable thermal emission in a hybrid metal-optical tamm state structure," *ACS Photonics*, Vol. 7, No. 6, 1569–1576, June 17, 2020, doi: 10.1021/acsphotonics.0c00439.

19. Giannini, V., G. Vecchi, and J. Gómez Rivas, "Lighting up multipolar surface plasmon polaritons by collective resonances in arrays of nanoantennas," *Physical Review Letters*, Vol. 105, No. 26, 266801, December 20, 2010, doi: 10.1103/PhysRevLett.105.266801.

20. Gokhale, V. J., P. D. Myers, and M. Rais-Zadeh, "Subwavelength plasmonic absorbers for spectrally selective resonant infrared detectors," *SENSORS, 2014 IEEE*, 982–985, November 2–5, 2014, doi: 10.1109/ICSENS.2014.6985167.

21. Aydin, K., V. E. Ferry, R. M. Briggs, and H. A. Atwater, "Broadband polarization-independent resonant light absorption using ultrathin plasmonic super absorbers," *Nature Communications*, Vol. 2, No. 1, 517, November 1, 2011, doi: 10.1038/ncomms1528.

22. Xing, Y., B. Urasinska-Wojcik, and J. W. Gardner, "Plasmonic enhanced CMOS non-dispersive infrared gas sensor for acetone and ammonia detection," *2018 IEEE International Instrumentation and Measurement Technology Conference (I2MTC)*, 1–5, May 14–17, 2018, doi: 10.1109/I2MTC.2018.8409745.

23. Su, P., Z. Han, D. Kita1, P. Becla, H. Lin, S. Deckoff-Jones1, K. Richardson, L. C. Kimerling, J. Hu, and A. Agarwal, "Monolithic on-chip mid-IR methane gas sensor with waveguide-integrated detector," *Applied Physics Letters*, Vol. 114, No. 5, 051103, 2019, doi: 10.1063/1.5053599.

24. Jin, T., J. Zhou, H.-Y. G. Lin, and P. T. Lin, "Mid-infrared chalcogenide waveguides for real-time and nondestructive volatile organic compound detection," *Analytical Chemistry*, Vol. 91, No. 1, 817–822, January 2, 2019, doi: 10.1021/acs.analchem.8b03004.

25. Park, J. H., S. E. Han, P. Nagpal, and D. J. Norris, "Observation of thermal beaming from tungsten and Molybdenum Bull's eyes," *ACS Photonics*, Vol. 3, No. 3, 494–500, March 16, 2016, doi: 10.1021/acsphotonics.6b00022.

26. Herriott, D. R., H. Kogelnik, and R. Kompfner, "Off-axis paths in spherical mirror interferometers," *Appl. Opt.*, Vol. 3, 523–526, 1964.

27. McManus, J. B., P. L. Kebabian, and W. S. Zahniser, "Astigmatic mirror multipass absorption cells for long-path-length spectroscopy," *Applied Optics*, Vol. 34, No. 18, 3336–3348, June 1995, doi: 10.1364/ao.34.003336.

28. Ozharar, S. and A. Sennaroglu, "Mirrors with designed spherical aberration for multi-pass cavities," *Opt. Lett.*, Vol. 42, No. 10, 1935–1938, May 2017, doi: 10.1364/ol.42.001935.

29. Cao, Y. N., G. Cheng, X. Tian, G.-S. Wang, Y. Cao, C.-Y. Sun, Y.-L. Zhang, G.-X. Cheng, and H.-T. Yang, "The design and simulation of a novel ring multi-pass optical cell for detection of environmental trace gas," *Optik*, Vol. 227, Art No. 166095, February 2021, doi: 10.1016/j.ijleo.2020.166095.

30. Nadeem, F., J. Mandon, A. Khodabakhsh, S. M. Cristescu, and F. J. M. Harren, "Sensitive spectroscopy of acetone using a widely tunable external-cavity quantum cascade laser," *Sensors*, Vol. 18, No. 7, 2050, 2018, online available: https://www.mdpi.com/1424-8220/18/7/2050.

31. Xia, J., F. Zhu, A. A. Kolomenskii, J. Bounds, S. Zhang, M. Amani, L. J. Fernyhough, and H. A. Schuessler, "Sensitive acetone detection with a mid-IR interband cascade laser and wavelength modulation spectroscopy," *OSA Continuum*, Vol. 2, No. 3, 640–654, March 15, 2019, doi: 10.1364/OSAC.2.000640.

32. Schwarm, K. K., C. L. Strand, V. A. Miller, and R. M. Spearrin, "Calibration-free breath acetone sensor with interference correction based on wavelength modulation spectroscopy near 8.2 µm," *Applied Physics B*, Vol. 126, No. 1, 9, December 9, 2019, doi: 10.1007/s00340-019-7358-x.

33. Lindley, R. E., M. Pradhan, and A. J. Orr-Ewing, "Measuring acetylene concentrations using a frequency chirped continuous wave diode laser operating in the near infrared," *Analyst*, Vol. 131, No. 6, 731–738, 2006, doi: 10.1039/B600506C.

34. Zou, M., Z. Yang, L. Sun, and X. Ming, "Acetylene sensing system based on wavelength modulation spectroscopy using a triple-row circular multi-pass cell," *Opt. Express*, Vol. 28, No. 8, 11573–11582, April 13, 2020, doi: 10.1364/OE.388343.

35. Shen, F., J. Akil, Gaoxuan Wang, C. Poupin, R. Cousin, S. Siffert, E. Fertein, T.-N. Ba, and W. Chen, "Real-time monitoring of N2O production in a catalytic reaction process using mid-infrared quantum cascade laser," *Journal of Quantitative Spectroscopy and Radiative Transfer*, Vol. 221, 1–7, December 1, 2018, doi: https://doi.org/10.1016/j.jqsrt.2018.09.022.

36. He, H., S. Gao, J. Hu, T. Zhang, T. Wu, Z. Qiu, C. Zhang, Y. Sun, and S. He 4, "In-situ testing of methane emissions from landfills using laser absorption spectroscopy," *Applied Sciences*, Vol. 11, No. 5, 2117, 2021, online available: https://www.mdpi.com/2076-3417/11/5/2117.

37. Herbelin, J. M., J. A. McKay, M. A. Kwok, R. H. Ueunten, D. S. Urevig, D. J. Spencer, and D. J. Benard, "Sensitive measurement of photon lifetime and true reflectances in an optical cavity by a phase-shift method," *Appl. Opt.*, Vol. 19, No. 1, 144–147, January 1, 1980, doi: 10.1364/AO.19.000144.

38. Anderson, D. Z., J. C. Frisch, and C. S. Masser, "Mirror reflectometer based on optical cavity decay time," *Appl. Opt.*, Vol. 23, No. 8, 1238, April 15, 1984 (in English), doi: 10.1364/ao.23.001238.

39. O'Keefe, A. and D. A. G. Deacon, "Cavity ring-down optical spectrometer for absorption measurements using pulsed laser sources," *Review of Scientific Instruments*, Vol. 59, No. 12, 2544–2551, 1988, doi: 10.1063/1.1139895.

40. Song, S., "Continuous-wave cavity ring-down spectroscopy and detection of trace methane," *Fine Mechanics and Physics*, University of Chinese Academy of Sciences 2019.

41. Parkes, A. M., R. E. Lindley, and A. J. Orr-Ewing, "Combining preconcentration of air samples with cavity ring-down spectroscopy for detection of trace volatile organic compounds in the atmosphere," *Analytical Chemistry*, Vol. 76, No. 24, 7329–7335, December 1, 2004, doi: 10.1021/ac048727j.

42. Pradhan, M., R. E. Lindley, R. Grilli, I. R. White, D. Martin, and A. J. Orr-Ewing, "Trace detection of C2H2 in ambient air using continuous wave cavity ring-down spectroscopy combined with sample pre-concentration," *Applied Physics B*, Vol. 90, No. 1, 1–9, 2008, doi: 10.1007/s00340-007-2833-1.

43. Wang, C. and A. B. Surampudi, "An acetone breath analyzer using cavity ringdown spectroscopy: an initial test with human subjects under various situations," *Measurement Science and Technology*, Vol. 19, No. 10, 105604, August 27, 2008, doi: 10.1088/0957-0233/19/10/105604.

44. Bicer, A., J. Bounds, F. Zhu, A. A. Kolomenskii, N. Kaya, E. Aluauee, M. Amani, and H. A. Schuessler, "Sensitive spectroscopic analysis of biomarkers in exhaled breath," *International Journal of Thermophysics*, Vol. 39, No. 6, 69, April 19, 2018, doi: 10.1007/s10765-018-2389-9.

45. Sadiek, I., Q. Shi, D. W. R. Wallace, and G. Friedrichs, "Quantitative mid-infrared cavity ringdown detection of methyl iodide for monitoring applications," *Analytical Chemistry*, Vol. 89, No. 16, 8445–8452, August 15, 2017, doi: 10.1021/acs.analchem.7b01970.

46. Wang, Z., M. Sun, and C. Wang, "Detection of melanoma cancer biomarker dimethyl disulfide using cavity ringdown spectroscopy at 266 nm," *Appl. Spectrosc.*, Vol. 70, No. 6, 1080-5, June 2016 (in English), doi: 10.1177/0003702816641575.

47. Parkes, A. M., B. L. Fawcett, R. E. Austin, S. Nakamichi, D. E. Shallcross, and A. J. Orr-Ewing, "Trace detection of volatile organic compounds by diode laser cavity ring-down spectroscopy," *Analyst* Vol. 128, No. 7, 960–965, 2003, doi: 10.1039/B303834C.

48. Vaittinen, O., F. M. Schmidt, M. Metsala, and L. Halonen, "Exhaled breath biomonitoring using laser spectroscopy," *Current Analytical Chemistry*, Vol. 9, No. 3, 463–475, 2013, doi: http://dx.doi.org/10.2174/1573411011309030016.

49. Schmidt, F. M., O. Vaittinen, M. Metsälä, P. Kraus, and L. Halonen, "Direct detection of acetylene in air by continuous wave cavity ring-down spectroscopy," *Applied Physics B: Lasers and Optics*, Vol. 101, 671–682, November 1, 2010, doi: 10.1007/s00340-010-4027-5.

50. Thalman, R. and R. Volkamer, "Inherent calibration of a blue LED-CE-DOAS instrument to measure iodine oxide, glyoxal, methyl glyoxal, nitrogen dioxide, water vapour and aerosol extinction in open cavity mode," *Atmos. Meas. Tech.*, Vol. 3, No. 6, 1797–1814, 2010, doi: 10.5194/amt-3-1797-2010.

51. Ball, S. M., J. M. Langridge, and R. L. Jones, "Broadband cavity enhanced absorption spectroscopy using light emitting diodes," *Chemical Physics Letters*, Vol. 398, No. 1, 68–74, November 1, 2004, doi: https://doi.org/10.1016/j.cplett.2004.08.144.

52. Fiedler, S. E., A. Hese, and A. A. Ruth, "Incoherent broad-band cavity-enhanced absorption spectroscopy of liquids," *Review of Scientific Instruments*, Vol. 76, No. 2, 023107, 2005, doi: 10.1063/1.1841872.

53. Fiedler, S. E., A. Hese, and A. A. Ruth, "Incoherent broad-band cavity-enhanced absorption spectroscopy," *Chemical Physics Letters*, Vol. 371, 284–294, 2003.

54. Islam, M., L. Ciaffoni, G. Hancock, and G. A. D. Ritchie, "Demonstration of a novel laser-driven light source for broadband spectroscopy between 170 nm and 2.1 μm," *Analyst*, Vol. 138, No. 17, 4741–4745, 2013, doi: 10.1039/C3AN01020A.

55. Seetohul, L. N., Z. Ali, and M. Islam, "Liquid-phase broadband cavity enhanced absorption spectroscopy (BBCEAS) studies in a 20 cm cell," *Analyst*, Vol. 134, No. 9, 1887–1895, 2009, doi: 10.1039/B907316G.

56. Wu, T., W. Chen, E. Fertein, F. Cazier, D. Dewaele, and X. Gao, "Development of an open-path incoherent broadband cavity-enhanced spectroscopy based instrument for simultaneous measurement of HONO and NO2 in ambient air," *Applied Physics B*, Vol. 106, No. 2, 501–509, February 1, 2012, doi: 10.1007/s00340-011-4818-3.

57. Denzer, W., M. L. Hamilton, G. Hancock, M. Islam,c C. E. Langley, R. Peverall, and G. A. D. Ritchie, "Near-infrared broad-band cavity enhanced absorption spectroscopy using a superluminescent light emitting diode," *Analyst*, Vol. 134, No. 11, 2220–2223, 2009, doi: 10.1039/B916807A.

58. Chandran, S. and R. Varma, "Near infrared cavity enhanced absorption spectra of atmospherically relevant ether-1, 4-Dioxane," *Spectrochim Acta A. Mol. Biomol. Spectrosc.*, Vol. 153, 704-8, January 15, 2016 (in English), doi: 10.1016/j.saa.2015.09.030.

59. Denzer, W., G. Hancock, M. Islam, C. E. Langley, R. Peverall, G. A. D. Ritchie, and D. Taylor, "Trace species detection in the near infrared using Fourier transform broadband cavity enhanced absorption spectroscopy: Initial studies on potential breath analytes," *Analyst*, Vol. 136, No. 4, 801–806, 2011, doi: 10.1039/C0AN00462F.

60. Amiot, C., A. Aalto, P. Ryczkowski, J. Toivonen, and G. Genty, "Cavity enhanced absorption spectroscopy in the mid-infrared using a supercontinuum source," *Applied Physics Letters*, Vol. 111, No. 6, 061103, 2017, doi: 10.1063/1.4985263.

61. Fang, B., W. Zhao, X. Xu, J. Zhou, X. Ma, S. Wang, W. Zhang, D. S. Venables, and W. Chen, "Portable broadband cavity-enhanced spectrometer utilizing Kalman filtering: application to real-time, in situ monitoring of glyoxal and nitrogen dioxide," *Opt. Express*, Vol. 25, No. 22, 26910–26922, October 30 2017, doi: 10.1364/OE.25.026910.

62. Chen, J., J. C. Wenger, and D. S. Venables, "Near-ultraviolet absorption cross sections of nitrophenols and their potential influence on tropospheric oxidation capacity," *The Journal of Physical Chemistry A*, Vol. 115, No. 44, 12235–12242, November 10, 2011, doi: 10.1021/jp206929r.

63. Yi, H., et al., "Intercomparison of IBBCEAS, NitroMAC and FTIR analyses for HONO, NO2 and CH2O measurements during the reaction of NO2 with H2O vapour in the simulation chamber CESAM," *Atmos. Meas. Tech.*, Vol. 14, No. 8, 5701–5715, 2021, doi: 10.5194/amt-14-5701-2021.

64. Meng, L., G. Wang, P. Augustin, M. Fourmentin, Q. Gou, E. Fertein, T. N. Ba, C. Coeur, A. Tomas, and W. Chen, "Incoherent broadband cavity enhanced absorption spectroscopy (IBBCEAS)-based strategy for direct measurement of aerosol extinction in a lidar blind zone," *Opt. Lett.*, Vol. 45, No. 7, 1611–1614, April 1, 2020, doi: 10.1364/OL.389093.

65. Miklós, A., P. Hess, and Z. Bozóki, "Application of acoustic resonators in photoacoustic trace gas analysis and metrology," *Review of Scientific Instruments*, Vol. 72, No. 4, 1937–1955, 2001, doi: 10.1063/1.1353198.

66. Dumitras, D. C., M. Petrus, A.-M. Bratu, and C. Popa, "Applications of near infrared photoacoustic spectroscopy for analysis of human respiration: A review," *Molecules*, Vol. 25, No. 7, 1728, 2020, online available: https://www.mdpi.com/1420-3049/25/7/1728.

67. Harren, F., J. Mandon, and S. M. Cristescu, *Photoacoustic Spectroscopy in Trace Gas Monitoring*, 2012.

68. J. Li, W. Chen, and B. Yu, "Recent Progress on Infrared Photoacoustic Spectroscopy Techniques," *Applied Spectroscopy Reviews*, Vol. 46, No. 6, 440-471, 2011/08/01 2011, doi: 10.1080/05704928.2011.570835.

69. Patimisco, P., G. Scamarcio, F. Tittel, and V. Spagnolo, "Quartz-enhanced photoacoustic spectroscopy: A review," *Sensors (Basel, Switzerland)*, Vol. 14, 6165–206, April 1, 2014, doi: 10.3390/s140406165.

70. Popa, C. L., A. M. Bratu, and M. Petrus, "A comparative photoacoustic study of multi gases from human respiration: Mouth breathing vs. nasal breathing," *Microchemical Journal*, 2018.

71. Mitrayana, D., K. Apriyanto, and M. Satriawan, "CO2 laser photoacoustic spectrometer for measuring acetone in the breath of lung cancer patients," *Biosensors*, Vol. 10, No. 6, 55, 2020, online available: https://www.mdpi.com/2079-6374/10/6/55.

72. Mohebbifar, M. R., "High-sensitivity detection and quantification of CHCl3 vapors in various gas environments based on the photoacoustic spectroscopy," *Microwave and Optical Technology Letters*, Vol. 61, No. 9, 2234–2241, 2019, doi: https://doi.org/10.1002/mop.31880.

73. Wang, G., T. Zhang, Y. Jiang, and S. He, "Compact photoacoustic spectrophone for simultaneously monitoring the concentrations of dichloromethane and trichloromethane with a single acoustic resonator," *Opt Express*, Vol. 30, No. 5, 7053–7067, February 28, 2022 (in English), doi: 10.1364/oe.450685.

74. Zhang, T., Y. Xing, G. Wang, and S. He, "High sensitivity continuous monitoring of chloroform gas by using wavelength modulation photoacoustic spectroscopy in the near-infrared range," *Applied Sciences*, Vol. 11, No. 15, 6992, 2021. online available: https://www.mdpi.com/2076-3417/11/15/6992.

75. Ma, Y., R. Lewicki, M. Razeghi, and F. K. Tittel, "QEPAS based ppb-level detection of CO and N2O using a high power CW DFB-QCL," *Opt. Express*, Vol. 21, No. 1, 1008–1019, January 14, 2013, doi: 10.1364/OE.21.001008.

76. Ayache, D., W. Trzpil, R. Rousseau, K. Kinjalk, R. Teissier, A. N. Baranov, M. Bahriz, and A. Vicet, "Benzene sensing by quartz enhanced photoacoustic spectroscopy at 14.85 μm," *Opt. Express*, Vol. 30, No. 4, 5531–5539, February 14, 2022, doi: 10.1364/OE.447197.

77. Ma, Y., Y. He, Y. Tong, X. Yu, and F. K. Tittel, "Quartz-tuning-fork enhanced photothermal spectroscopy for ultra-high sensitive trace gas detection," *Opt. Express*, Vol. 26, No. 24, 32103–32110, November 26, 2018, doi: 10.1364/OE.26.032103.

78. Lang, Z., S. Qiao, and Y. Ma, "Acoustic microresonator based in-plane quartz-enhanced photoacoustic spectroscopy sensor with a line interaction mode," *Opt. Lett.*, Vol. 47, No. 6, 1295–1298, March 15, 2022, doi: 10.1364/OL.452085.

79. Liu, X. and Y. Ma, "Sensitive carbon monoxide detection based on light-induced thermoelastic spectroscopy with a fiber-coupled multipass cell (invited)," *Chinese Optics Letters*, Vol. 20, No. 3, 031201, 2022, doi: 10.3788/col202220.031201.

80. Tomberg, T., M. Vainio, T. Hieta, and L. Halonen, "Sub-parts-per-trillion level sensitivity in trace gas detection by cantilever-enhanced photo-acoustic spectroscopy," *Scientific Reports*, Vol. 8, No. 1, 1848, January 30, 2018, doi: 10.1038/s41598-018-20087-9.

81. Karhu, J., H. Philip, A. Baranov, R. Teissier, and T. Hieta, "Sub-ppb detection of benzene using cantilever-enhanced photoacoustic spectroscopy with a long-wavelength infrared quantum cascade laser," *Opt. Lett.*, Vol. 45, No. 21, 5962–5965, November 1, 2020, doi: 10.1364/OL.405402.

82. Hirschmann, C. B., N. S. Koivikko, J. Raittila, J. Tenhunen, S. Ojala, K. Rahkamaa-Tolonen, R. Marbach, S. Hirschmann, and R. L. Keiski, "FT-IR-cPAS–new photoacoustic measurement technique for analysis of hot gases: A case study on VOCs," *Sensors (Basel)*, Vol. 11, No. 5, 5270–5289, 2011 (in English), doi: 10.3390/s110505270.

83. Saalberg, Y., H. Bruhns, and M. Wolff, "Photoacoustic spectroscopy for the determination of lung cancer biomarkers — A preliminary investigation," *Sensors*, Vol. 17, No. 1, 210, 2017, online available: https://www.mdpi.com/1424-8220/17/1/210.

84. Bacsik, Z., J. Mink, and G. Keresztury, "FTIR Spectroscopy of the Atmosphere. I. Principles and Methods," *Applied Spectroscopy Reviews*, Vol. 39, No. 3, 295–363, December 31, 2004, doi: 10.1081/ASR-200030192.

85. Lechner, B., H. Paar, and P. Sturm, "Measurement of VOCs in vehicle exhaust by extractive FTIR spectroscopy," *Europto Remote Sensing. SPIE*, 2001.

86. Cantu, A., G. Pophal, S. Hall, and C. T. Laush, "A unique application of an extractive FTIR ambient air monitoring system for the simultaneous detection of multiple-ppb-level VOCs," *Applied Physics B: Lasers and Optics*, Vol. 67, 493–496, October 1, 1998, doi: 10.1007/s003400050534.

87. Fathy, A., Y. M. Sabry, M. Amr, et al., "MEMS FTIR optical spectrometer enables detection of volatile organic compounds (VOCs) in part-per-billion (ppb) range for air quality monitoring," *SPIE OPTO*, 2019.

88. Cheng, J., Y. Zhang, T. Wang, P. Norris, W.-Y. Chen, and W.-P. Pan, "Thermogravimetric-fourier transform infrared spectroscopy-gas chromatography/mass spectrometry study of volatile organic compounds from coal pyrolysis," *Energy & Fuels*, Vol. 31, No. 7, 7042–7051, July 20, 2017, doi: 10.1021/acs.energyfuels.7b01073.

89. Flores, E., R. Basaldud, and M. Grutter, "Open-path FTIR spectroscopic studies of trace gases over mexico city," *Journal of Extension*, 2003.

90. Hong, D. W., G. S. Heo, J. S. Han, and S. Y. Cho, "Application of the open path FTIR with COL1SB to measurements of ozone and VOCs in the urban area," *Atmospheric Environment*, Vol. 38, No. 33, 5567–5576, October 1, 2004, doi: https://doi.org/10.1016/j.atmosenv.2004.06.033.

91. Lin, C., N. Liou, and E. Sun, "Applications of open-path fourier transform infrared for identification of volatile organic compound pollution sources and characterization of source emission behaviors," *Journal of the Air & Waste Management Association*, Vol. 58, No. 6, 821–828, June 1, 2008, doi: 10.3155/1047-3289.58.6.821.

92. Russwurm, G. M., R. H. Kagann, O. A. Simpson, W. A. McClenny, and W. F. Herget, "Long-path FTIR measurements of volatile organic compounds in an industrial setting," *Journal of the Air & Waste Management Association*, Vol. 41, No. 8, 1062–1066, 1991.

93. Sedlmaier, A., K. Schafer, K. H. Becker, K. Brockmann, J. Heland, R. Kurtenbach, J. Lorzer, and P. Wiesen, "Determination of VOCs in traffic exhaust by FTIR absorption spectrometry," *Industrial Lasers and Inspection (EUROPTO Series). SPIE*, 1999.

94. Li, Y., J. Wang, Z. Huang, and X. Zhou, "Mapping air contaminant concentrations using remote sensing FTIR," *Journal of Environmental Science and health. Part A, Toxic/hazardous Substances & Environmental Engineering*, Vol. 38, No. 2, 429–38, February 2003 (in English), doi: 10.1081/ese-120016905.

95. Tong, J.-J., W.-Q. Liu, M.-G. Gao, Z.-M. Liu, L. Xu, X.-L. Wei, and L. Jin, "Measurement and study of partial VOCs based on open path FTIR," *5th International Symposium on Advanced Optical Manufacturing and Testing Technologies: Optical Test and Measurement Technology and Equipment*, Vol. 7656, 76562B, Y. Zhang, J. Sasián, L. Xiang, and S. To, editors, October 1, 2010, doi: 10.1117/12.863726, online available: https://ui.adsabs.harvard.edu/abs/2010SPIE.7656E..2BT.

96. Han, X., L. Jin, M. Gao, S. Ye, L. Xu, Y. Li, R. Hu, M. Feng, and W. Liu, "The study of VOCs emission monitoring technology based on SOF-FTIR," *Light, Energy and the Environment 2015*, paper EW2A.5, OSA Technical Digest (online) (Optica Publishing Group), 2015, https://doi.org/10.1364/EE.2015.EW2A.5.

97. Buszewski, B., M. Kesy, T. Ligor, and A. Amann, "Human exhaled air analytics: biomarkers of diseases," *Biomed Chromatogr*, Vol. 21, No. 6, 553–566, June 2007 (in English), doi: 10.1002/bmc.835.

98. Tomberg, T., N. Vuorio, T. Hieta, et al., "Broadband laser-based infrared detector for gas chromatography," *Analytical Chemistry*, Vol. 92, No. 21, 14582–14588, November 3, 2020, doi: 10.1021/acs.analchem.0c02887.

99. Zare, R. N., D. S. Kuramoto, C. Haase, S. M. Tan, E. R. Crosson, and N. M. Saad, "High-precision optical measurements of 13C/12C isotope ratios in organic compounds at natural abundance," *Proc. Natl. Acad. Sci. U S A*, Vol. 106, No. 27, 10928-32, July 7, 2009 (in English), doi: 10.1073/pnas.0904230106.